Diffractive cross sections at HERA and diffractive PDFs

Laurent Schoeffel[a] (on behalf of the H1 and ZEUS collaborations)

[a] CEA Saclay, Irfu/SPP, 91191 Gif-sur-Yvette Cedex, France

A large collection of results for the diffractive dissociation of virtual photons, $\gamma^\star p \to Xp$, have been obtained with the H1 and ZEUS detectors at HERA. Different experimental techniques have been used, by requiring a large rapidity gap between X and the outgoing proton, by analyzing the mass distribution, M_X, of the hadronic final state, as well as by directly tagging the proton. A reasonable compatibility between those techniques and between H1 and ZEUS results have been observed. Some common fundamental features in the measurements are also present in all data sets. They are detailed in this document. Diffractive PDFs can give a good account of those features. Ideas and results are discussed in the following.

1. Experimental diffraction at HERA

One of the most important experimental results from the DESY ep collider HERA is the observation of a significant fraction of events in Deep Inelastic Scattering (DIS) with a large rapidity gap (LRG) between the scattered proton, which remains intact, and the rest of the final system. This fraction corresponds to about 10% of the DIS data at $Q^2 = 10$ GeV^2. In DIS, such events are not expected in such abundance, since large gaps are exponentially suppressed due to color string formation between the proton remnant and the scattered partons. Events are of the type $ep \to eXp$, where the final state proton carries more than 95 % of the proton beam energy. A photon of virtuality Q^2, coupled to the electron (or positron), undergoes a strong interaction with the proton (or one of its low-mass excited states Y) to form a hadronic final state system X of mass M_X separated by a LRG from the leading proton (see Fig. 1). These events are called diffractive. In such a reaction, $ep \to eXp$, no net quantum number is exchanged, and the longitudinal momentum fraction $1 - x_{I\!P}$ is lost by the proton. Thus, the longitudinal momentum $x_{I\!P}P$ is transferred to the system X. In addition to the standard DIS kinematic variables and $x_{I\!P}$, a diffractive event is also often characterized by the variable $\beta = x_{Bj}/x_{I\!P}$, which takes a simple interpretation in the parton model discussed in the following.

Experimentally, a diffractive DIS event, $ep \to eXp$, is presented in Fig. 2 (bottom). The dissociating particle is the virtual photon emitted by the electron. The final state consists of the scattered electron and hadrons which populate the photon fragmentation region. The proton is scattered in the direction of the initial beam proton with little change in momentum and angle. In particular, we detect no hadronic activity in the direction of the proton flight, as the proton remains intact in the diffractive process. On the

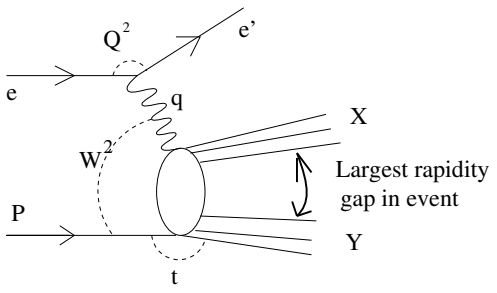

Figure 1. Illustration of the process $ep \to eXY$. The hadronic final state is composed of two distinct systems X and Y, which are separated by the largest interval in rapidity between final state hadrons.

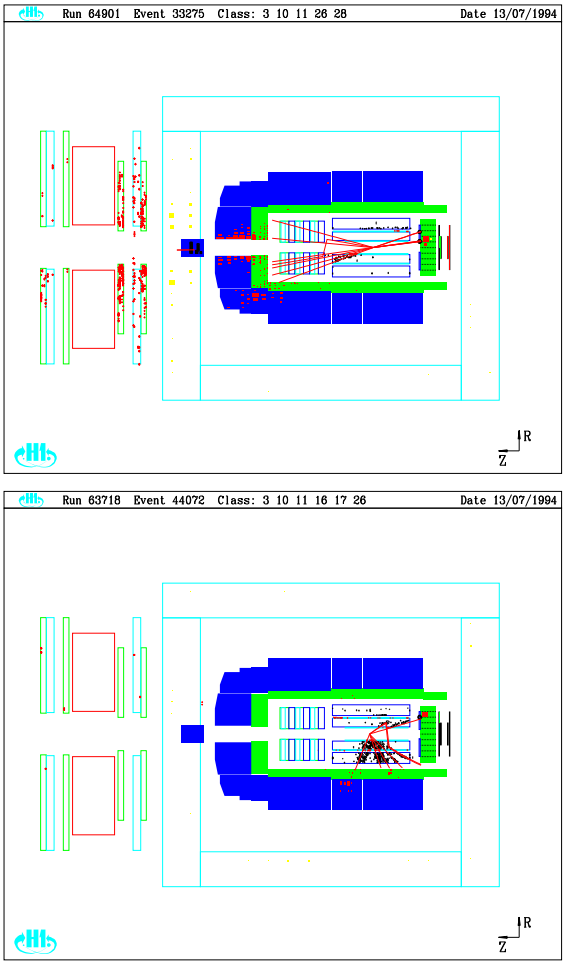

Figure 2. Usual (top) and diffractive (bottom) events in the H1 experiment at HERA. For a diffractive event, no hadronic activity is visible in the the proton fragmentation region, as the proton remains intact in the diffractive process. On the contrary, for a standard DIS event, the proton is destroyed in the reaction, and the flow of hadronic clusters is clearly visible in the proton fragmentation region (+z direction, i.e. forward part of the detector).

contrary, for a standard DIS event (Fig. 2 top), the proton is destroyed in the reaction and the flow of hadronic clusters is clearly visible in the proton fragmentation region (forward part of the detector).

The experimental selection of diffractive events in DIS proceeds in two steps. Events are first selected based on the presence of the scattered electron in the detector. Then, for the diffractive selection itself, three different methods have been used at HERA:

1. A reconstructed proton track is required in the leading (or forward) proton spectrometer (LPS for ZEUS or FPS for H1) with a fraction of the initial proton momentum $x_L > 0.97$. Indeed, the cleanest selection of diffractive events with photon dissociation is based on the presence of a leading proton in the final state. By leading proton we mean a proton which carries a large fraction of the initial beam proton momentum. This is the cleanest way to select diffractive events, but the disadvantage is a reduced kinematic coverage.

2. The hadronic system X measured in the central detector is required to be separated by a large rapidity gap from the rest of the hadronic final state. This is a very efficient way to select diffractive events in a large kinematic domain, close to the standard DIS one. The prejudice is a large background as discussed in the following.

3. The diffractive contribution is identified as the excess of events at small M_X above the exponential fall-off of the non-diffractive contribution with decreasing $\ln M_X^2$. The exponential fall-off, expected in QCD, permits the subtraction of the non-diffractive contribution and therefore the extraction of the diffractive contribution without assuming the precise M_X dependence of the latter. This is also a very efficient way to select diffractive events in a large kinematic domain.

Extensive measurements of diffractive DIS cross sections have been made by both the ZEUS and

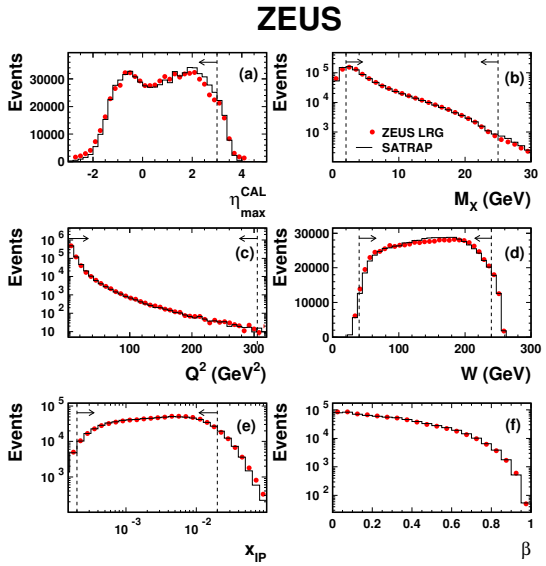

Figure 3. Comparison of the distributions of data (dots) to those obtained with the Monte-Carlo (histograms) for typical variables in the LRG analysis.

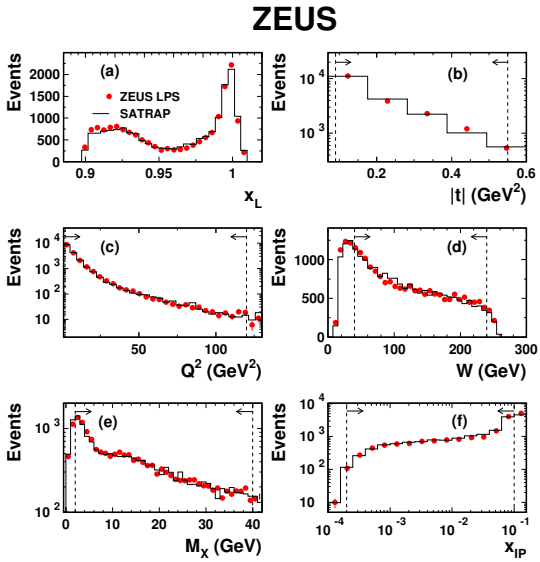

Figure 4. Comparison of the distributions of data (dots) to those obtained with the Monte-Carlo (histograms) for typical variables in the LPS analysis.

H1 collaborations at HERA, using different experimental techniques [1–5]. Of course, the comparison of these techniques provides a rich source of information to get a better understanding of the experimental gains and prejudices of those techniques. In Fig. 3 and 4, the basis of the last ZEUS experimental analysis is summarized [5]. Data are compared to Monte-Carlo (MC) expectations for typical variables. The MC is based on specific models for signal and backgrounds, and the good agreement with data is proof that the main ingredients of the experimental analysis are under control: resolutions, calibrations, efficiencies... These last sets of data (Fig. 3 and 4) [5] contain five to seven times more statistics than in preceding publications of diffractive cross sections, and thus opens the way to new developments in data/models comparisons. A first relative control of the data samples is shown in Fig. 5, where the ratio of the diffractive cross sections is displayed, as obtained with the LPS and the LRG experimental techniques. The mean value of the ratio of 0.86 indicates that the LRG sample contains about 24% of proton-dissociation background, which is not present in the LPS sample. This background corresponds to events like $ep \to eXY$, where Y is a low-mass excited state of the proton (with $M_Y < 2.3$ GeV). It is obviously not present in the LPS analysis which can select specifically a proton in the final state. This is the main background in the LRG analysis. Due to a lack of knowledge of this background, it causes a large normalisation uncertainty of 10 to 15% for the cross sections extracted from the LRG analysis. We can then compare the results obtained by the H1 and ZEUS experiments for diffractive cross sections in Fig. 6, using the LRG method. A good compatibility of both data sets is observed, after rescaling the ZEUS points by a global factor of 13%. This factor is compatible with the normalisation uncertainty described above. We can also compare the results obtained by the H1 and ZEUS experiments in Fig. 7, using the tagged proton method (LPS for ZEUS and

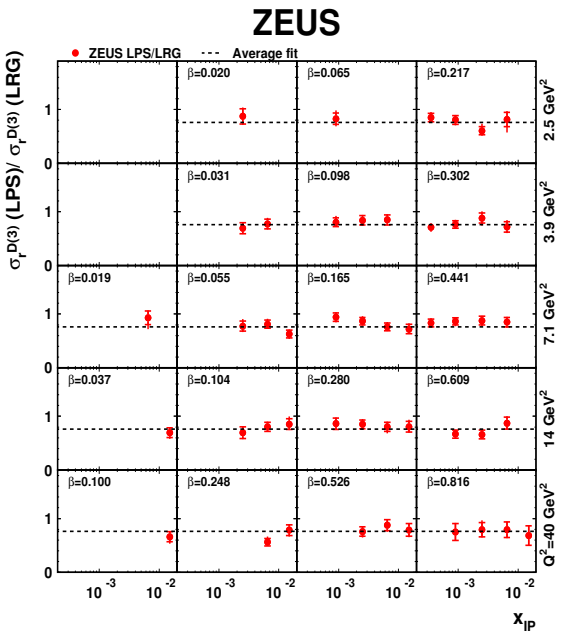

Figure 5. Ratio of the diffractive cross sections, as obtained with the LPS and the LRG experimental techniques. The lines indicate the average value of the ratio, which is about 0.86. It implies that the LRG sample contains about 24% of proton dissociation events, corresponding to processes like $ep \to eXY$, where $M_Y < 2.3$ GeV. This fraction is approximately the same for H1 data (of course in the same M_Y range).

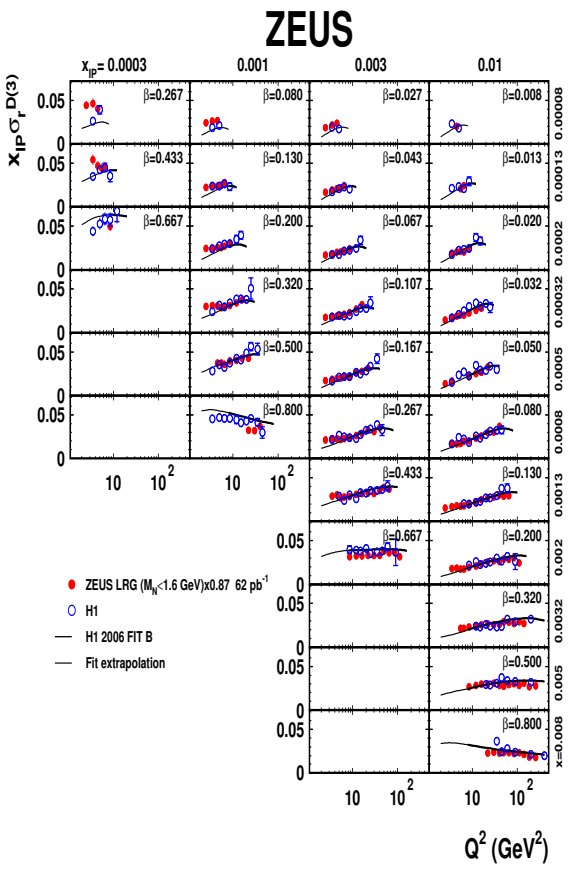

Figure 6. The diffractive cross sections obtained with the LRG method by the H1 and ZEUS experiments. The ZEUS values have been rescaled (down) by a global factor of 13%. This value is compatible with the normalisation uncertainty of this sample.

FPS for H1). In this case, there is no proton dissociation background and the diffractive sample is expected to be clean. It gives a good reference to compare both experiments. A global normalisation difference of about 10% can be observed in Fig. 7, which can be studied with more data. It remains compatible with the normalisation uncertainty for this tagged proton sample. It is interesting to note that the ZEUS measurements are globally above the H1 data by about 10% for both techniques, tagged proton or LRG. In Fig. 8, we compare the results using the LRG and the M_X methods, for ZEUS data alone. Both sets are in good agreement, which shows that there is no strong bias between these experimental techniques. The important message at this level is not only the observation of differences as illustrated in Fig. 6 and 7, but the opportunity opened with the large statistics provided by the ZEUS measurements. Understanding discrepancies between data sets is part of the experimental challenge of the next months. It certainly needs analysis of new data sets from the H1 experiment. However, already at the present level, much can be done with existing data for the understanding of diffraction at HERA.

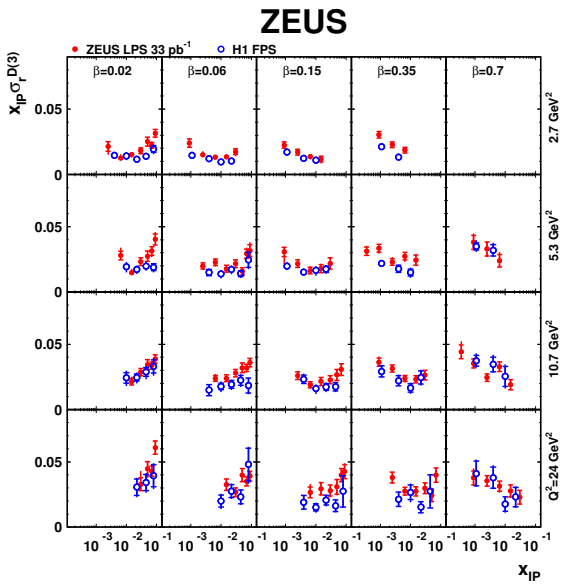

Figure 7. The diffractive cross section obtained with the FPS (or LPS) method by the H1 and ZEUS experiments, where the proton is tagged. The ZEUS measurements are above H1 by a global factor of about 10%.

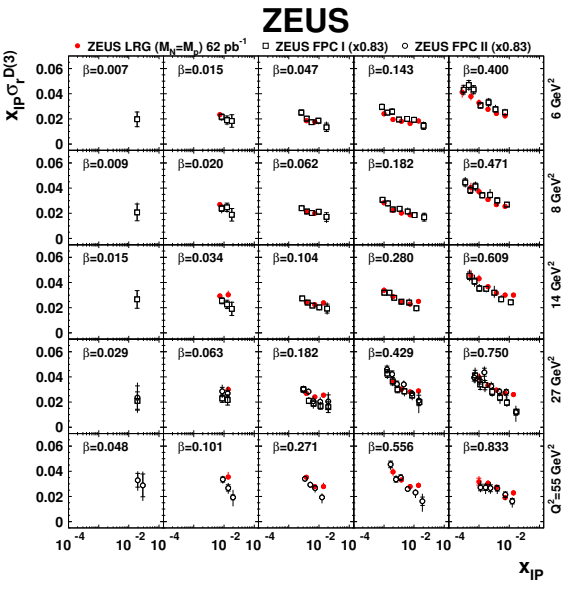

Figure 8. The diffractive cross sections obtained with the LRG method (full dots) compared with the results obtained with the M_X method (open symbols: FPC I and FPC II). All values are converted to $M_Y = M_p$.

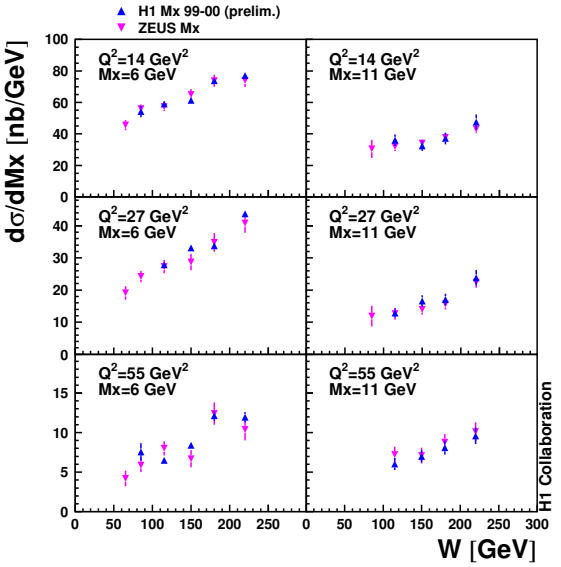

Figure 9. Cross sections of the diffractive process $\gamma^* p \to p' X$, differential in the mass of the diffractively produced hadronic system X (M_X), are presented as a function of the center-of-mass energy of the $\gamma^* p$ system W. Measurements at different values of the virtuality Q^2 of the exchanged photon are displayed. We observe a behavior of the form $\sim W^{0.6}$ for the diffractive cross section, compatible with the dependence expected for a hard process.

2. Diffractive PDFs at HERA

In order to compare diffractive data with perturbative QCD models, or parton-driven models, the first step is to show that the diffractive cross section shows a hard dependence in the centre-of-mass energy W of the $\gamma^* p$ system. In Fig. 9, we observe a behavior of the form $\sim W^{0.6}$, compatible with the dependence expected for a hard process. This observation is obviously the key to allow further studies of the diffractive process in the context of perturbative QCD. Events with diffractive topology can be studied in terms of the Pomeron trajectory exchanged between the proton and the virtual photon. In this view, these events result from a colour-singlet exchange between the diffractively dissociated virtual photon and the proton (see Fig. 10).

A diffractive structure function $F_2^{D(3)}$ can then be defined as a sum of two factorized contributions, corresponding to a Pomeron and secondary Reggeon trajectories:

$$F_2^{D(3)}(Q^2,\beta,x_{I\!P}) = f_{I\!P/p}(x_{I\!P})F_2^{D(I\!P)}(Q^2,\beta) + f_{I\!R/p}(x_{I\!P})F_2^{D(I\!R)}(Q^2,\beta)\,,$$

where $f_{I\!P/p}(x_{I\!P})$ is the Pomeron flux. It depends only on $x_{I\!P}$, once integrated over t, and $F_2^{D(I\!P)}$ can be interpreted as the Pomeron structure function, depending on β and Q^2. The other function, $F_2^{D(I\!R)}$, is an effective Reggeon structure function taking into account various secondary Regge contributions which cannot be separated. The Pomeron and Reggeon fluxes are assumed to follow a Regge behavior with linear trajectories $\alpha_{I\!P,I\!R}(t) = \alpha_{I\!P,I\!R}(0) + \alpha'_{I\!P,I\!R}t$, such that

$$f_{I\!P/p,I\!R/p}(x_{I\!P}) = \int_{t_{cut}}^{t_{min}} \frac{e^{B_{I\!P,I\!R}t}}{x_{I\!P}^{2\alpha_{I\!P,I\!R}(t)-1}}\mathrm{d}t\,,$$

where $|t_{min}|$ is the minimum kinematically allowed value of $|t|$, and $t_{cut} = -1$ GeV^2 is the limit of the measurement. We take $\alpha'_{I\!P} = 0.06$ GeV^{-2}, $\alpha'_{I\!R} = 0.30$ GeV^{-2}, $B_{I\!P} = 5.5$ GeV^{-2} and $B_{I\!R} = 1.6$ GeV^{-2}. The Pomeron intercept $\alpha_{I\!P}(0)$ is left as a free parameter in the QCD fit and $\alpha_{I\!R}(0)$ is fixed to 0.50.

The next step is then to model the Pomeron structure function $F_2^{D(I\!P)}$ [1,7–9]. Among the most popular models, the one based on a point-like structure of the Pomeron has been studied extensively, using a non-perturbative input supplemented by a perturbative QCD evolution equations [7–9]. In this formulation, it is assumed that the exchanged object, the Pomeron, is a colour-singlet quasi-particle whose structure is probed in the DIS process. As for standard DIS, diffractive parton distributions related to the Pomeron can be derived from QCD fits to diffractive cross sections. The procedure is standard: we assign parton distribution functions to the Pomeron parametrised in terms of non-perturbative input distributions at some low scale Q_0^2. The quark flavor singlet distribution ($zS(z,Q^2) = u + \bar{u} + d + \bar{d} + s + \bar{s}$) and the gluon distribution ($zG(z,Q^2)$) are parametrised at this initial scale Q_0^2, where

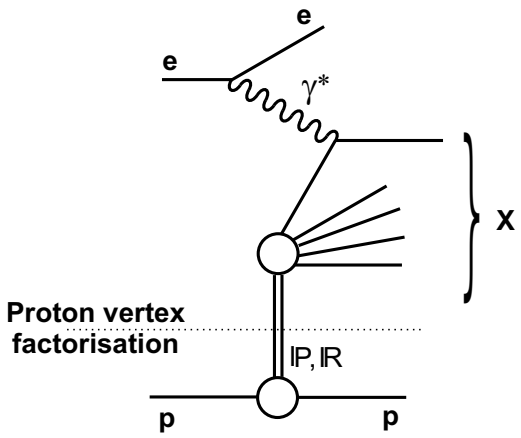

Figure 10. Schematic diagram of a diffractive process. Events with a diffractive topology can be studied in terms of the Pomeron trajectory exchanged between the proton and the virtual photon.

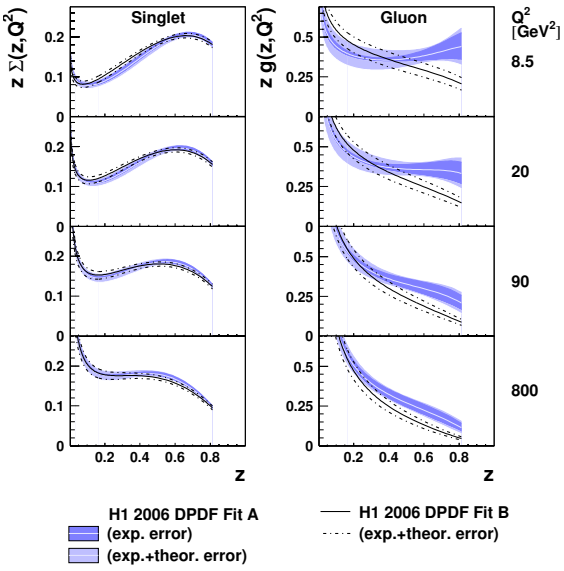

Figure 11. Singlet and gluon distributions of the Pomeron (DPDFs) as a function of $z \equiv \beta$, the fractional momentum of the Pomeron carried by the struck parton (see text), obtained by a QCD fit to the H1 diffractive cross sections.

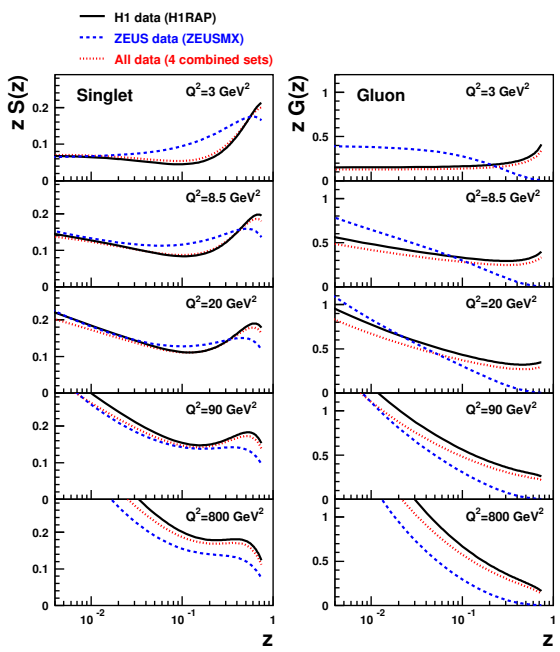

Figure 12. Singlet and gluon DPDFs as a function of $z \equiv \beta$, where the results of fitting H1 or ZEUS data are compared. The ZEUS data considered here [3] are derived using the M_X method. A global fit of all published data is also presented. Note that the last ZEUS data set [5] is not used for this plot.

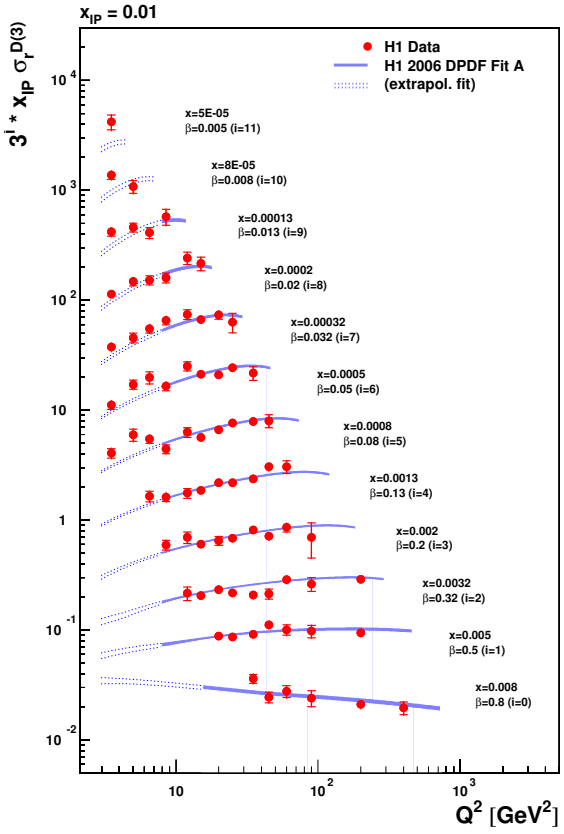

Figure 13. Scaling violations for H1 diffractive cross sections for one value of $x_{I\!P}$ ($x_{I\!P} = 0.01$) and a large range of β values, from low (< 0.01) to large values (> 0.5).

$z = x_{i/I\!P}$ is the fractional momentum of the Pomeron carried by the struck parton. Functions zS and zG are evolved to higher Q^2 using the next-to-leading order DGLAP evolution equations. For the structure of the sub-leading Reggeon trajectory, the pion structure function [6] is assumed with a free global normalization to be determined by the data. Diffractive PDFs (DPDFs) extracted from H1 and ZEUS data are shown in Fig. 11 and 12 [1,7–9]. We observe that some differences in the data are reflected in the DPDFs, but some basic features are common for all data sets and the resulting DPDFs. Firstly, the gluon density is larger than the sea quark density, which means that the major fraction of the momentum (about 70%) is carried by the gluon for a typical value of $Q^2 = 10$ GeV^2. Secondly, we observe that the gluon density is quite large at large β, with a large uncertainty, which means that we expect positive scaling violations still at large values of β. This is shown in Fig. 13. We note that even at large values of $\beta \sim 0.5$, the scaling violations are still positive, as discussed above. The strength of the DPDFs approach is to give a natural interpretation of this basic observation and to describe properly the Q^2 evolution of the cross sections. Other approaches are also well designed to describe all features of the data [12], but this is another story. The near future of the study of DPDFs is to combine all existing data and check their compatibility with respect to

the QCD fit technique. If this is verified, a new global analysis can be followed to get the most complete understanding of DPDFs [7].

3. Diffractive PDFs and the LHC

Note that diffractive distributions are process-independent functions. They appear not only in inclusive diffraction but also in other processes where diffractive hard-scattering factorization holds. The cross section of such a process can be evaluated as the convolution of the relevant parton-level cross section with the DPDFs. For instance, the cross section for charm production in diffractive DIS can be calculated at leading order in α_s from the $\gamma^* g \to c\bar{c}$ cross section and the diffractive gluon distribution. An analogous statement holds for jet production in diffractive DIS. Both processes have been analyzed at next-to-leading order in α_s and are found to be consistent with the factorization theorem [10]. A natural question to ask is whether one can use the DPDFs extracted at HERA to describe hard diffractive processes such as the production of jets, heavy quarks or weak gauge bosons in $p\bar{p}$ collisions at the Tevatron. Fig. 14 shows results on diffractive dijet production from the CDF collaboration compared to the expectations based on the DPDFs from HERA [11]. The discrepancy is spectacular: the fraction of diffractive dijet events at CDF is a factor 3 to 10 smaller than would be expected on the basis of the HERA data. The same type of discrepancy is consistently observed in all hard diffractive processes in $p\bar{p}$ events. In general, while at HERA hard diffraction contributes a fraction of order 10% to the total cross section, it contributes only about 1% at the Tevatron. This observation of QCD-factorization breaking in hadron-hadron scattering can be interpreted as a survival gap probability or a soft color interaction which needs to be considered in such reactions. In fact, from a fundamental point of view, diffractive hard-scattering factorization does not apply to hadron-hadron collisions. Attempts to establish corresponding factorization theorems fail, because of interactions between spectator partons of the colliding hadrons. The contribution of these interactions to the cross section does not decrease with the hard scale. Since they are not associated with the hard-scattering subprocess, we no longer have factorization into a parton-level cross section and the parton densities of one of the colliding hadrons. These interactions are generally soft, and we have at present to rely on phenomenological models to quantify their effects [11]. The yield of diffractive events in hadron-hadron collisions is then lowered precisely because of these soft interactions between spectator partons (often referred to as reinteractions or multiple scatterings). They can produce additional final-state particles which fill the would-be rapidity gap (hence the often-used term rapidity gap survival). When such additional particles are produced, a very fast proton can no longer appear in the final state because of energy conservation. Diffractive factorization breaking is thus intimately related to multiple scattering in hadron-hadron collisions. Understanding and describing this phenomenon is a challenge in the high-energy regime that will be reached at the LHC [13]. We can also remark sim-

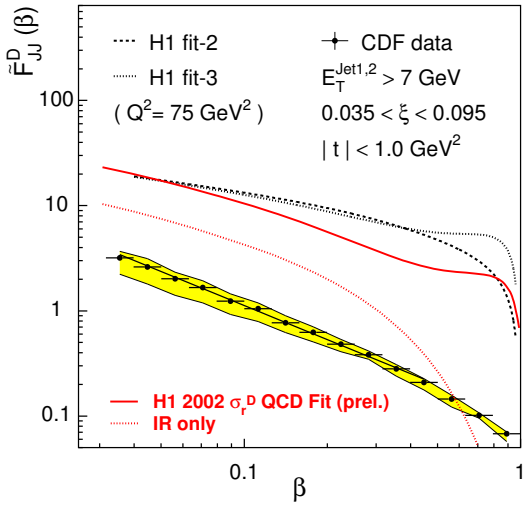

Figure 14. Comparison between the CDF measurement of the diffractive structure function (black points) with the H1 diffractive PDFs.

ply that the collision partners, in pp or $p\bar{p}$ reactions, are both composite systems of large transverse size, and it is not too surprising that multiple interactions between their constituents can be substantial. In contrast, the virtual photon in $\gamma^* p$ collisions has small transverse size, which disfavors multiple interactions and enables diffractive factorization to hold. According to our discussion, we may expect that for decreasing virtuality Q^2 the photon behaves more and more like a hadron, and diffractive factorization may again be broken.

4. Conclusions

We have presented and discussed the most recent results on inclusive diffraction from the HERA experiments. A large collection of data sets and diffractive cross sections are published, which present common fundamental features in all cases. The different experimental techniques, for both H1 and ZEUS experiments, provide compatible results, with still some global normalization differences of about 10%. DPDFs give a good account of the main features of the diffractive data. There is still much to do on the experimental side with large statistics analyses, in order to obtain a better understanding of data and backgrounds. This is an essential task for the next months with the purpose to understand and reduce the normalisation uncertainties of diffractive measurements at HERA. This will make the combination of cross sections between the two experiments much easier, with a common message from HERA on inclusive diffraction.

REFERENCES

1. A. Aktas *et al.* [H1 Collaboration], Eur. Phys. J. C **48** (2006) 715 [arXiv:hep-ex/0606004].
2. A. Aktas *et al.* [H1 Collaboration], Eur. Phys. J. C **48** (2006) 749 [arXiv:hep-ex/0606003].
3. S. Chekanov *et al.* [ZEUS Collaboration], Nucl. Phys. B **713** (2005) 3 [arXiv:hep-ex/0501060].
4. S. Chekanov *et al.* [ZEUS Collaboration], Eur. Phys. J. C **38** (2004) 43 [arXiv:hep-ex/0408009].
5. M. Ruspa *et al.* [ZEUS Collaboration], [arXiv:hep-ex/0808.0833].
6. J.F. Owens, Phys. Rev. D **30** (1984) 943.
7. C. Royon, L. Schoeffel, S. Sapeta, R.B. Peschanski and E. Sauvan, Nucl. Phys. B **781** (2007) 1 [arXiv:hep-ph/0609291].
8. C. Royon, L. Schoeffel, R.B. Peschanski and E. Sauvan, Nucl. Phys. B **746** (2006) 15 [arXiv:hep-ph/0602228].
9. C. Royon, L. Schoeffel, J. Bartels, H. Jung and R. B. Peschanski, Phys. Rev. D **63** (2001) 074004 [arXiv:hep-ph/0010015].
10. J.C. Collins, Phys. Rev. D **57** (1998) 3051 [Erratum-ibid. D **61** (2000) 019902] [arXiv:hep-ph/9709499].
11. T. Affolder *et al.* [CDF Collaboration], Phys. Rev. Lett. **84** (2000) 5043.
12. C. Marquet and L. Schoeffel, Phys. Lett. B **639** (2006) 471.
13. AFP TDR in ATLAS to be submitted; see: `http://project-rp220.web.cern.ch/project-rp220`.